Diffusion-weighted MRI for differential diagnosis of pulmonary tuberculosis-like lesions:A pilot study

Qinqin Yan
Shanghai Public Health Clinical Center
Shuihua Lu
Shanghai Public Health Clinical Center
Tao Li
Shanghai Public Health Clinical Center
Jie Shen
Shanghai Public Health Clinical Center
Mengxiao Liu
: Siemens Healthcare Limited
Robert Grimm
Siemens Healthcare GmbH
Fei Shan
Shanghai Public Health Clinical Center
Zhiyong Zhang
Zhongshan Hospital Fudan University
Yuxin Shi (shiyx828288@163.com)
Fudan University https://orcid.org/0000-0001-5181-2023

Research

Keywords: MRI, tuberculosis, malignancy, non-tuberculosis benign lesions, differential diagnosis

Posted Date: March 30th, 2021

DOI: https://doi.org/10.21203/rs.3.rs-348020/v1

Abstract

Background

To investigate the value of 3T magnetic resonance imaging (MRI) diffusion-weighted and intro-voxel incoherent motion imaging (DWI-IVIM) in differential diagnosis of tuberculosis-like lesions.

Methods

78 patients with 99 lesions comprised of 36 tuberculosis (TB), 38 pulmonary malignancy (PM), 25 non-tuberculosis benign lesions (NTB) underwent 3T-MRI examination, including star-volumetric interpolated breath-hold examination (Star-VIBE), fast-BLADE turbo spin echo (fBLADE TSE), DWI-IVIM (b = 0,30,50,80,100,200,400,600,800,1000 s/mm2). Signal ratio (SR) of lesions to rhomboid muscle, apparent diffusion coefficients (ADCs) and IVIM D, D* and f values were compared using *Mann-Whitney U* test. The sensitivity, specificity and accuracy were obtained via the receptor operative curve (ROC). Delong test was used for comparisons of ROCs.

Results

Compared to Mg, the T2SR of TB was statistically significantly lower, with AUC of 0.67[*95%CI*: 0.55–0.78]. ADCs and IVIM D of TB was evidently higher, with pooled sensitivity of 73.7–84.6%, pooled specificity of 80.2–86.1% and pooled accuracy of 81.1–83.8%. $ADC_{(0,1000)}$ combined with D improved AUC from 0.85 to 0.91. Comparisons of T1SR, D* and f had no differences. As for TB vs. NTB, ADCs had pooled sensitivity of 44.4–69.4%, pooled specificity of 80.0–96.0% and pooled accuracy of 63.9–75.4%. The sensitivity and specificity of D* were 77.8% and 60.0%. IVIM coupled with ADC further revealed no diagnostic improvement. T1SR, T2SR, IVIM D and f had no statistical differences.

Conclusion

T2SR, DWI and IVIM can distinguish tuberculosis-like lesions. The clinical use of pulmonary MRI is extremely suitable for the elderly and immunocompromised patients with pulmonary tuberculosis.

Introduction

Pulmonary TB is ranked as the one of the top ten causes of death in the worldwide, which is generally susceptible in all age groups from infancy to the elderly, especially for those with malnutrition, immunocompromised, and smoking history. There were about 10 million new TB patients in the worldwide in 2018, with women and children (≤15 years old) accounting for 32% and 11% respectively. Among the elderly and immunodeficiency patients with pulmonary TB, the incidence of co-existent lung

cancer and opportunistic infections evidently grow[1–6]. The definite diagnosis came to priority in the management of tuberculosis.

Chest computer tomography (CT) and x-ray are historically used for evaluation of pulmonary lesions, which are usually harmful due to cumulative radiation exposure, especially for children, the pregnant and young women. Previous studies have reported that cumulative radiation exceed 100mSv caused an increased cancer mortality risk[7–8]. It is also quite difficult for radiologists to distinguish TB from malignancy or other infectious diseases by means of morphology and subjective observation. MRI has advantages such as non-radiation, functional measurements and so on, which is suitable for recurrent examinations and qualitative diagnosis of lesions. DWI and IVIM, based on inherent diffusion motion of water, are clinically used for differential diagnosis of benign and malignant lesions, which also had great diagnostic value for suspicious pulmonary nodules. Shen and his colleagues reported a pooled sensitivity of 0.84 (95%CI: 0.82–0.86) and pooled specificity of 0.84 (95%CI: 0.81–0.87) in identifying pulmonary malignancy using DWI[9]. IVIM D of malignancy was significantly lower than benign pulmonary lesions[10, 11], while the diagnostic value of IVIM D* and f value were controversial[12–14]. Generally, MRI is available to differentiate pulmonary malignancy and benign lesions, however, it is still unknown about discrimination among pulmonary tuberculosis-like lesions, which was hardly ever reported previously.

In this study, DWI ADCs and IVIM parameters (D, D* and f values) were obtained based on mono-exponential and bi-exponential respectively. The diagnostic performances of MRI DWI and IVIM were compared between pulmonary tuberculosis and malignancy, tuberculosis and non-tuberculosis benign lesions. The preliminary study was expected to be helpful for differential diagnosis of granulomatous disease and clinical management of tuberculosis.

Subject And Methods

1.1 Subjects and clinical data

A total of 106 patients underwent 3T-MRI examination from October 2018 to January 2020 in Shanghai Public Health Clinical Center (International Review Board, IRB, 2019-S021-02) in this prospective study. Patients who meet the criteria as follows were enrolled: a. pulmonary lesions with pathological and/or laboratory test evidences, b. no contraindications for MRI. The exclusion criteria included: a. in-definite lesions, b. pulmonary malignancy after chemotherapy or radiotherapy, c. being uncooperative to complete MRI examination. 28 patients were excluded for that 20 of them had no pathological or laboratory test evidences, 4 of them had mixed pattern of tuberculosis and fungal infection, 4 of them had chemotherapy and/or radiotherapy history. Finally, 78 patients (female: 23, male: 55, mean age: 56±12 years) with a total of 99 lesions were enrolled which consisted of 16 squamous carcinomas, 15 adenocarcinomas, 4 neuroendocrine tumors, 1 diffuse large B-cell lymphoma, 2 metastasis, 36 tuberculosis, 1 non-tuberculosis mycobacterium infection, 2 granulomatous vasculitis, 14 fungal infections, 7 organizing pneumonia, 1 lung abscess. The work-flow was listed as Figure 1. According to the pathological and/or laboratory test evidences, all lesions were divided into three groups including PM

(n=38), TB (n=36) and NTB (n=25). The PM consisted of 34 nodules/masses, 1 consolidation and 3 cavities. The TB included 29 nodules/masses, 1 consolidation and 6 cavities. And the NTB had 22 nodules/masses, 1 consolidation and 2 cavities. The average size of lesions was (2.6±1.6)cm, rang from 0.7cm to 7.8cm.

1.2 MRI protocol

All patients underwent MRI examination using 3T whole-body MR scanner (MAGNETOM Skyra, Siemens Healthcare, Erlangen, Germany) with an 18-element body wrap coil. All parameters was listed as follows: axial T1-weighted StarVIBE: TR/TE=2.79/1.39 ms, thickness: 2mm, field of view (FOV): 380mm. T2-weighted fBLADE TSE: TR/TE=1870/69 ms, thickness: 3mm, FOV: 380mm. EPI-DWI: TR/TE: 4000/49 ms, thickness: 4mm, FOV: 380mm, b=0, 30, 50, 80, 100, 200, 400, 600, 800, 1000. All patients underwent respiratory training before performing MRI examination. And a diagram navigation was used for DWI scan.

2.3 CT scan

All patients underwent examination on CT 320-detector system (Aquilion Vision, Canon Medical Systems, Japan) in the case of breath-holding after inspiration. The following imaging parameters were applied: detector width, 80 x 0.5 mm; pitch, 0.813; tube voltage, 120 kV; automatic tube current with SD 10 (Sure Exp 3D set, maximum: 440 mA, minimum: 60 mA). All CT images with 1 mm contiguous section thickness were reconstructed by means of adaptive iterative dose-reduction with three-dimensional processing (AIDR 3D, standard) and a high frequency reconstruction algorithm (FC56) for the lung window setting, and with a standard reconstruction algorithm (FC17) for the mediastinum window setting. The lung window width and level were adjusted appropriately by the reference standards of 1,600 and 600 Hounsfield unit (Hu). The imaging volume was from the pulmonary apex to the costophrenic angle.

2.4 Data postprocessing

Firstly, using serial thin-section CT images as references, the morphology of lesions was documented in MRI images. The signal ratio in T1WI (T1SR) and T2WI (T2SR) images was calculated as the ratio of the lesions' signal intensity (SI) to the rhomboid muscular signal. All ROIs were the same pixel. The formula listed as: $SR= SI_{lesions} / SI_{muscular}$. The hyper-intensity in this study was described as the SR more than 1, otherwise, it was hypo-intensity.

Then, the raw data was imported to the body diffusion toolbox (Siemens, Germany) for acquiring ADC values and IVIM D, D* and f values. The measurements were performed by 2 radiologists respectively with 3- and 6- years experiences of chest radiographs, who were blind to patients' clinical data. And two post-processing experts employed by the Siemens company helped supervise the data-analysis. Using T2WI images as references, $ADC_{(0,600)}$ (b=0,600 s/mm2), $ADC_{(0,800)}$ (b=0,800 s/mm2) and $ADC_{(0,1000)}$ (b=0,1000 s/mm2) were obtained in a basis of DWI model. IVIM D, D* and f value were calculated with IVIM model (b=0,30,50,80,100,200,400,600,800,1000 s/mm2). The region of interests (ROIs) were manually drawn on the three slices with less motion artifacts and large-scale and then were averaged. ROIs area were more than 50% of lesions at least. And all ROIs should avoid air and necrosis as much as possible.

2. **Statistical analysis**

MedCalc 15.2.2 was used for data analysis. The inter-class correlation coefficient (ICC) was used for assessing inter-observer agreement. A *Mann-Whitney U test* was used for comparisons of ADC-values, IVIM parameters and signal ratio in T1WI/T2WI images between TB and PM, TB and NTB. *P*-value 0.05 was defined as statistical differences. Multi-parameters logistic regression was used for analyzing the combined diagnostic efficacy of IVIM and ADC. The diagnostic efficacy was obtained based on receptor operative characteristics (ROC). A maximum Youden's index was used for determining the cut-off value, sensitivity, specificity and accuracy. A Delong-test was used for comparisons of area under the curve (AUC).

Results

3.1 MRI findings

3T-MRI is comparable to CT in detecting lobular sign (n=56/57, 98.2%), spiculation (n=9/9, 100%), bronchiectasis (n=17/20, 85.0%), pleural indentation (n=18/20, 90.0%) and satellite lesion (n=3/4, 75.0%). The T1SR in PM, TB and NTB were (1.09±0.16), (1.07±0.19) and (1.01±0.24) respectively. 68.4% (n=26/38) of PM showed slightly hyper-intensity in T1WI StarVIBE and 100% showed hyper-intensity in T2WI fBLADE TSE images. 69.4% (n=25/36) of TB was slightly hyper-intensity in T1WI StarVIBE and 77.8% (n=28/36) was slightly hyper-intensity in T2WI images. 44.0% (n=11/25) of NTB was slightly hyper-intensity in T1WI StarVIBE and 84.0% (n=21/25) was hyper-intensity in T2WI images. Comparisons of T1SR between PM and TB, TB and NTB had no significantly differences (*P* 0.05). The T2SR in TB (1.87±0.92) was statistically lower than PM (2.43±1.09) (*P*=0.01), with AUC of 0.67 [95%CI: 0.55-0.78]. The sensitivity, specificity and cut-off value were 79.0%, 55.6% and 1.74. T2SR of NTB was 1.92±0.90, with no statistical difference in comparison of TB (*P* 0.05) (Table 1.). Figure 2. showed the MRI manifestation of tuberculoma.

3.2 ICCs of ADCs and IVIM parameters

ICCs of $ADC_{(0,600)}$, $ADC_{(0,800)}$ and $ADC_{(0,1000)}$ were 0.98, 0.97, 0.98 respectively. ICCs of IVIM D, D* and f values were 0.98, 0.90 and 0.87 respectively.

3.3 Comparisons between TB and PM

4.3.1 ADCs results

As shown in the Table 2. ADCs (eg. $ADC_{(0,600)}$) in TB was significantly higher than PM and the differences were statistically significant (P<0.01). Comparisons of ROCs for ADCs had no statistical significance (P>0.05). The $ADC_{(0,800)}$ and $ADC_{(0,1000)}$ had the same highest AUC of 0.85 [0.76-0.94], and the accuracy of 82.4%. The highest specificity was 86.1% separately in $ADC_{(0,600)}$ and $ADC_{(0,800).}$ And the best sensitivity was 84.6% in $ADC_{(0,1000)}$. The diagnostic performances of ADCs were presented with Table 3.

4.3.2 IVIM results

The D* in TB and PM were (19.00±12.35) x 10-3mm2/s and (16.07±7.13) x 10-3mm2/s. And the f-value were (0.261±0.131) and (0.210±0.116) respectively. There is no statistical significance in D* and f-value, when compared TB and PM. D-value in PM was significantly lower than TB [(0.88±0.26) x 10-3 mm2/s versus (1.26±0.31) x 10-3 mm2/s] (P<*0.01*), with cut-off value of 1.01 x 10-3 mm2/s. The sensitivity, specificity accuracy and AUC were 78.9%, 83.3%, 81.1% and 0.85 [95%CI:0.75-0.92] separately. Combination of $ADC_{(0,1000)}$ and IVIM D value for identifying TB and PM acquired an improved AUC of 0.91 [95%CI:0.82-0.97]. The sensitivity, specificity and accuracy were 94.7%, 72.2% and 83.3% respectively.

4.4 Comparisons between TB and NTB

4.4.1 ADCs results

$ADC_{(0,600)}$, $ADC_{(0,800)}$ and $ADC_{(0,1000)}$ in NTB were statistically higher than TB (P<0.01). There was no statistical differences in comparisons of ROCs in ADCs (eg. $ADC_{(0,600)}$) (P>0.05) (Table 4.). The $ADC_{(0,800)}$ had the highest AUC of 0.73 [95%CI: 0.60-0.86]. The sensitivity, specificity and accuracy were 69.4%, 84.0% and 75.4% separately. The highest specificity of 96.0% existed in $ADC_{(0,1000)}$. (Table 5.) (Figure 3.).

4.4.2 IVIM results

The D-value in TB and NTB were (1.26±0.31) x 10-3mm2/s and (1.39±0.23) x 10-3mm2/s. The f-value were (0.261±0.131) and (0.289±0.140) respectively. There was no statistically significance in D and f-value, when compared TB with NTB (*P>0.05*). D* value of TB was statistically lower than NTB [(19.00±12.35) x 10-3 mm2/s versus. (26.64±13.11) x 10-3 mm2/s] (*P=0.024*). The cut-off value was 22.83 x 10-3 mm2/s, with sensitivity of 77.8%, specificity of 60.0%, and AUC of 0.69[95%CI:0.55-0.80] separately. Combination of $ADC_{(0,1000)}$ and D* had no improvement in discrimination (*P>0.05*) (Figure 4.)

Discussion

In this study, we noted that 3T-MRI is comparable to thin-section CT for morphology of pulmonary lesions. Our previous studies also verified that free-breathing T1WI StarVIBE and T2WI fBLADE TSE were alternative for chest imaging, both with high signal noise ratio (SNR) and contrast noise ratio(CNR)[15]. Additionally, in terms of specially pathological caseous necrosis in TB[16–17], T2WI MRI is optimal for identifying such tuberculoma, which typically showed central lower intensity with peripherally ring-like higher intensity. Reasonably, T2SR of TB was evidently lower than lung cancer in this study. It is consistent with previous results[18–20], which reported that more cases showed hyper-intensity in T1WI images and hypo-intensity in T2WI images in tuberculoma with statistical significance, when compared to lung cancer. However, in this study, no evident difference of T1SR existed in TB and PM. We assumed that optional T1WI Dixon with in-out phase images would be more promising for differential diagnosis between tuberculoma and lung caner. Moreover, Comparisons of T2SR and T1SR between TB and NTB manifested no statistical difference, which has hardly been reported before.

The signal intensity of the tuberculoma were usually inhomogeneous because of inflammatory hyperplasia, caseous necrosis and liquefaction. Batra, et al.[26] reported that the T2WI signal intensity in tuberculoma was basically consistent with DWI signal intensity. Our results also manifested that 93.1% of tuberculoma (n = 29) had similar signal intensity in T2WI and DWI images, of which 51.7% (n = 15) was both hyper-intensity in T2WI and DWI images, 10.3% (n = 3) was both hypo-intensity, 31.0% (n = 9) was both central hypo-intensity with peripherally ring-like hyper-intensity, and 6.9% (n = 2) was central hypo-intensity with peripherally ring-like hyper-intensity in T2WI images while hyper-intensity in DWI images.

Functional MRI have been applied for differential pulmonary benign and malignant lesions. DWI ADC of lung cancer is significantly lower than benign lesions[10, 11, 21], with sensitivity of 80%-88%, and specificity of 89%-93%[22, 23]. In this study, ADCs of PM were significantly lower than tuberculosis, as previously reported. The $ADC_{(0,800)}$ and $ADC_{(0,1000)}$ obtained the same highest AUC of 0.85 [0.76–0.94], and the accuracy of 82.4%. While, the the total $ADC_{(0,800)}$ had more greater Youden index and less scan time, when compared with $ADC_{(0,1000)}$, which was optional for identifying TB and PM. All false negative cases in this group were lung adenocarcinoma (n = 6), mainly due to lower cell density and increased intracellular mucus[24, 25]. The ADCs [(1.30 ± 0.27) x 10 − 3 mm2/s] in adenocarcinoma was evidently higher than other malignancy [(0.83 ± 0.22) x 10 − 3 mm2/s] in this study.

IVIM parameters, especially for D* and f value, were controversial in the differential diagnosis of malignant and benign lesions[12, 13]. Our study demonstrated that IVIM D was valuable in identifying TB and PM, with sensitivity of 78.9%, specificity of 83.3% and accuracy of 81.1%. The performance of IVIM D not better than $ADC_{(0,1000)}$, which might attributed to motion artifacts interfering model fitting in a basis of multiple b values and long time. Also, a combination of IVIM D and $ADC_{(0,1000)}$ obviously improved the AUC from 0.85 to 0.91 and the sensitivity from 84.2–94.7%. Thus, a combination of IVIM D and $ADC_{(0,1000)}$ was recommend for differential diagnosis of TB and PM. However, IVIM D* and f in this study were of no use in distinguishing TB from lung caner.

Compared to TB, NTB such as fungal pneumonia, non-tuberculosis mycobacterial (NTM) infection and so on, have co-existent clinical and radiographic manifestations, which are difficult for discrimination, especially for elderly people with underlying diseases and HIV patients. MRI comparisons between TB and NTB have been hardly reported. In this study, there was significant difference in ADCs, when compared TB and NTB, of which $ADC_{(0,800)}$ was considerable for differential diagnosis. The sensitivity, specificity and accuracy were 69.4%, 84.0% and 75,4%. IVIM results also showed that IVIM D* in NTB was significantly higher than TB, with sensitivity of 77.8% and specificity of 60.0%. Caseous necrosis with reduced micro-circulation might be responsible for IVIM D* difference in TB and NTB. Yet, combination of IVIM D* and ADC acquired no improvement in diagnostic efficacy. And IVIM D and f can not be used for identifying TB and NTB.

Given of standard recommendation of the Fleischner Society[27], previous studies mainly focused on the differential diagnosis of pulmonary nodules over 8mm. However, imaging features such as nodules, consolidation and so on, all exist in tuberculosis, malignancy or other infectious disease, especially for those with co-existent tuberculosis-lung cancer and mixed infectious diseases. In this context, our inclusion enrolled a span of patients with pulmonary nodules, consolidation and cavity. However, there also were still some limitations in this study. Firstly, in view of this was a small sample study, additional cases were needed for reliability and repeatability. And the benign tumors were absent in present study. Secondly, more detailed grouping were expected, such as fungal infections group, benign tumor group and so on, especially for other infectious diseases. Lastly, our study explored the T2WI, DWI and IVIM features in tuberculosis and other infectious diseases. These results might cannot be extrapolated to areas in which granulomatous diseases are not endemic.

In conclusion, DWI and IVIM were helpful for differential diagnosis between TB and PM, TB and NTB. Additionally, T2WI signal intensity was also valuable in identifying TB and PM. The clinical use of pulmonary MRI is extremely suitable for the elderly and immunocompromised patients with pulmonary tuberculosis, who have high-risk of co-existent lung caner, opportunistic infections and tuberculosis.

Abbreviations

TB
tuberculosis

PM
pulmonary malignancy
NTB
non-tuberculosis benign lesions
CT
computed tomography
MRI
magnetic resonance imaging
DWI
diffusion-weighted imaging
IVIM
intro-voxel incoherent movement
ADC
apparent diffusion coefficient
T1SR
lesion signal to muscle signal ratio in T1-weighted image
T2SR
lesion signal to muscle signal ratio in T2-weighted image
ROI
region of interest
AUC
area under the curve
ICC
intra-class correlation coefficient
SNR
signal to noise ratio
CNR
contrast to noise ratio

Declarations

Ethics approval and consent to participate

This prospective study was approved by the ethical review board of Shanghai Public Health Clinical Center (2019-S021-02). and the informed consent has been sent to participants in this study.

Consent for publication

Not applicable

Availability of data and materials

The datasets generated and/or analyzed during the current study are not publicly available due privacy but are available from the corresponding author on reasonable request.

Competing interests

Non-financial competing interests must be declared in this section.

Funding

No funding

Authors' contributions

Conception and Design: YX S, ZY Z. Analysis and interpretation: QQ Y, SH L. Data Collection: QQ Y, T L, J S, F S. Critical reversion of the article: YX S, MX L, R G. Statistical analysis: QQ Y. Writing the article: QQ Y. MX L. and R G. are employed by a company in the medical industry. They supervised the data-analysis. All authors read and approved the final manuscript.

Acknowledges:

No applicable

References

1. Wong Jason YY, Zhang H, Hsiung Chao A, Kouya S., Chang YuKMatsuoKWongMPik,HYun-Chul,WJiucun,SWeiJWangZSongMKimHNam, Wei I-Shou,CNilanjan,Hu., Chen Wu., Tetsuya M., Wei Z., Adeline KJinHSeow., Caporaso Neil E, Yang SMin-Ho,CLapPAnShe-Juan,WPing,Y., Yasushi ZHong,Y., Qiuyin ZXu-Chao,KYoungTCai., Y Zhihua., K Young-Chul., Bassig Bryan A, Jiang C., Ho James Chung Man., Ji Bu-Tian., Daigo Yataro., I Hidemi., M Yukihide., A Kyota., K Yoichiro., H Takayuki., Hosgood H, Dean. S, Hiromi K Hideo., T Koji., WShun-Ichi,K Michiaki., M Yohei., N Haruhiko., M Shingo., T Masahiro., G Koichi., S Jianxin., S Lei., H Xing., T Atsushi., G Akiteru., M Yoshihiro., S Kimihiro., T Kazumi., W Fusheng., M Fumihiko., Su Jian., Kim Yeul Hong., Oh In-Jae., Song Fengju., Su Wu-Chou., Chen Yu-Min., Chang Gee-Chen., Chen Kuan-Yu., Huang Ming-Shyan.,

Chien Li-Hsin., Xiang Yong-Bing., Park Jae Yong., Kweon Sun-Seog., Chen Chien-Jen., Lee Kyoung-Mu., Blechter Batel., L Haixin., Gao Yu-Tang., Qian Biyun., Lu Daru., Liu Jianjun., Jeon Hyo-Sung., Hsiao Chin-Fu., Sung Jae Sook., Tsai Ying-Huang., Jung Yoo Jin., Guo Huan., Hu Zhibin., Wang Wen-Chang., Chung Charles C., Burdett Laurie., Yeager Meredith., Hutchinson Amy., Berndt Sonja, IWu Wei., PHerbert,LYuqing,CJin Eun., PK Hwa., SSookWLiuL, Kang, CH, Zhu Meng., CChung-Hsing,YTsung-Ying,XJun,GPeng,TWen,W Chih-Liang., Hsin Michael., Sit Ko-Yung., Ho James., Chen Ying., Choi Yi Young., Hung Jen-Yu., Kim Jun Suk., Yoon Ho Il., Lin Chien-Chung., Park In Kyu., Xu Ping., Wang Yuzhuo., He Qincheng., Perng Reury-Perng., Chen Chih-Yi., Vermeulen Roel., Wu Junjie., Lim Wei-Yen., Chen Kun-Chieh., Li Yao-Jen., Li Jihua., Chen Hongyan., Yu Chong-Jen., Jin Li., Chen Tzu-Yu., Jiang Shih-Sheng., Liu Jie., Y Taiki., H Belynda., W Kathleen., L Shengchao, A, Dai Juncheng., Ma Hongxia., Jin Guangfu., Song Bao., Wang Zhehai., Cheng Sensen., Li Xuelian., Ren Yangwu., Cui Ping., Iwasaki Motoki., Shimazu Taichi., Tsugane Shoichiro., Zhu Junjie., Chen Ying., Yang Kaiyun., Jiang Gening., Fei Ke., Wu Guoping., Lin Hsien-Chin., Chen Hui-Ling., Fang Yao-Huei., Tsai Fang-Yu., Hsieh Wan-Shan., Yu Jinming., Stevens Victoria L., Laird-Offringa Ite A., Marconett Crystal N., Rieswijk Linda., Chao Ann., Yang Pan-Chyr., Shu Xiao-Ou., Wu Tangchun., Wu Y L., Lin Dongxin., Chen Kexin., Zhou Baosen., Huang Yun-Chao., Kohno Takashi., Shen Hongbing., Chanock Stephen J., Rothman Nathaniel., Lan Qing.Tuberculosis infection and lung adenocarcinoma: Mendelian randomization and pathway analysis of genome-wide association study data from never-smoking Asian women. Genomics, 2020,112(2), 1223–1232.

2. Engels Eric A, Min S., Chapman Robert S, Pfeiffer Ruth M. Yu Ying-Ying., He Xingzhou., Lan Qing.Tuberculosis and subsequent risk of lung cancer in Xuanwei, China. Int J Cancer. 2009;124(5):1183–7.
3. Yu Ying-Ying, Pinsky Paul F, Caporaso Neil E, Nilanjan C., B Mona., L Patricia., Furuno Jon P, Lan Qing., Eric E A. Lung cancer risk following detection of pulmonary scarring by chest radiography in the prostate, lung, colorectal, and ovarian cancer screening trial. Arch Intern Med, 2008, 168(21), 2326-32.
4. Nalbandian A, Yan B-S, Pichugin A, Bronson RT, Kramnik I. Lung carcinogenesis induced by chronic tuberculosis infection: the experimental model and genetic control. Oncogene. 2009;28(17):1928–38.
5. Shiels Meredith S, Demetrius A., Jarmo V., Eric E. A. Increased risk of lung cancer in men with tuberculosis in the alpha-tocopherol, beta-carotene cancer prevention study. Cancer Epidemiol Biomarkers Prev. 2011;20(4):672–8.
6. Behr MA, Edelstein PH, Ramakrishnan L.. Is Mycobacterium tuberculosis infection life long? BMJ, 2019, 367.
7. United Nations Scientific Committee on the Effects. of Atomic Radiation Sources, effects and risks of ionizing radiation.2017, Last accessed on 08/07/2019.
8. Brambilla Marco V, Jenia K, Agnieszka, Rehani MM. Multinational data on cumulative radiation exposure of patients from recurrent radiological procedures: call for action. Eur Radiol. 2020;30:2493–501.

9. Shen Guohua M, Huan L, Bin R, Pengwei K, Anren. Diagnostic Performance of DWI With Multiple Parameters for Assessment and Characterization of Pulmonary Lesions: A Meta-Analysis. AJR Am J Roentgenol. 2018;210:58–67.
10. Liu Haidong., Ying L., Yu Tielian., Y Ning. Usefulness of diffusion-weighted MR imaging in the evaluation of pulmonary lesions. Eur Radiol, 2010.20(4), 807 – 15.
11. Çakmak Vefa U, Furkan K, Nevzat. Diffusion-weighted MRI of pulmonary lesions: Comparison of apparent diffusion coefficient and lesion-to-spinal cord signal intensity ratio in lesion characterization. J Magn Reson Imaging. 2017;45:845–54.
12. Yongxia DYu,LXinchun,L., Liang Changhong., Liu Zaiyi. Use of diffusion-weighted magnetic resonance imaging to distinguish between lung cancer and focal inflammatory lesions: a comparison of intravoxel incoherent motion derived parameters and apparent diffusion coefficient. Acta Radiol, 2016, 57(11), 1310–1317.
13. Wan Qi. Deng Ying-Shi., Zhou Jia-Xuan., Yu Yu-Dong., Bao Ying-Ying., Lei Qiang.,Chen Hou-Jin., Peng Ya-Hui., Mei Ying-Jie., Zeng Qing-Si., Li Xin-Chun. Intravoxel incoherent motion diffusion-weighted MR imaging in assessing and characterizing solitary pulmonary lesions. Sci Rep. 2017;7:43257.
14. Wang Li-li, Jiang L., Liu Kai., Chen Cai-zhong., Liu Hui., Lv Peng., Fu Cai-xia., Zeng Meng-su. Intravoxel incoherent motion diffusion-weighted MR imaging in differentiation of lung cancer from obstructive lung consolidation: comparison and correlation with pharmacokinetic analysis from dynamic contrast-enhanced MR imaging. Eur Radiol, 2014,24(8), 1914-22.
15. Shuyi YQinqin,Y., Jie S., Lu Shuihua., Shan Fei., Shi Yuxin. 3T magnetic resonance for evaluation of adult pulmonary tuberculosis. Int J Infect Dis, 2020,93, 287–294.
16. Yang Jin-Sun, Du Zhi-Xiang. Comparison of clinical and pathological features of lymph node tuberculosis and histiocytic necrotizing lymphadenitis. J Infect Dev Ctries, 2019, 13: 706–713.
17. Rizzi Elisa Busi., Schinina' Vincenzo., C Massimo., G Delia., P Fabrizio., B Nazario., Lauria Francesco N., Girardi Enrico., Bibbolino Corrado. Detection of Pulmonary tuberculosis: comparing MR imaging with HRCT. BMC Infect Dis 2011;11:243.
18. Damon NSebastianNKim., Tobias P., Ingo S, Sebastian GWyschkon., Hamm Bernd., Schwartz Stefan., Elgeti Thomas. Pulmonary MRI at 3T: Non-enhanced pulmonary magnetic resonance Imaging Characterization Quotients for differentiation of infectious and malignant lesions. Eur J Radiol, 2017, 89, 33–39.
19. Henz Concatto N, Watte G, Marchiori E, Irion K, Felicetti JC, Camargo JJ, Hochhegger B. Magnetic resonance imaging of pulmonary nodules: accuracy in a granulomatous disease-endemic region. Eur Radiol. 2016 Sep;26(9):2915–20.
20. Qi Li-Ping., Chen Ke-Neng., Zhou Xiaohong Joe., Tang Lei., Liu Yu-Liang., Li Xiao-Ting., Wang Juan., Sun Ying-Shi. Conventional MRI to detect the differences between mass-like tuberculosis and lung cancer. J Thorac Dis, 2018, 10(10), 5673–5684.
21. Mori Takeshi., Hiroaki N., I Koei., K Koichi., Shinya S., K Kazuhiro., Y Yasuyuki. Diffusion-weighted magnetic resonance imaging for diagnosing malignant pulmonary nodules/masses: comparison

with positron emission tomography. J Thorac Oncol, 2008, 3(4), 358 – 64.

22. Chen L, Z Jiuquan., B Jing., Lin Z., Xiaofei Hu., Xia Yunbao., Wang Jian. Meta-analysis of diffusion-weighted MRI in the differential diagnosis of lung lesions. J Magn Reson Imaging, 2013, 37(6), 1351-8.
23. Li B, L Qiong., C Cong., GYu,L Shiyuan. A systematic review and meta-analysis of the accuracy of diffusion-weighted MRI in the detection of malignant pulmonary nodules and masses. Acad Radiol, 2014, 21(1), 21 – 9.
24. Chen L, Yongfeng ZJiuquan,C., W Wenwei., Z Xiangdong., Yan Xiaochu., Wang Jian. Relationship between apparent diffusion coefficient and tumour cellularity in lung cancer. PLoS One, 2014, 9(6), e99865.
25. Matoba Munetaka., Hisao T., Tamaki K., Y Hajime., H Kotaro., Toga Hirohisa., Sakuma Tutomu. Lung carcinoma: diffusion-weighted mr imaging–preliminary evaluation with apparent diffusion coefficient. Radiology, 2007, 243(2), 570-7.
26. Batra A, Tripathi RP. Diffusion-weighted magnetic resonance imaging and magnetic resonance spectroscopy in the evaluation of focal cerebral tubercular lesions. Acta Radiol. 2004;45:679–88.
27. Macmahon H, Austin JHM, Gamsu G, Herold CJ, Swensen SJ. Guidelines for management of small pulmonary nodules detected on ct scans: a statement from the fleischner society 1. Radiology,2005, 237(2), 395–400.

Tables

Please see the supplementary files section to view the tables.

Figures

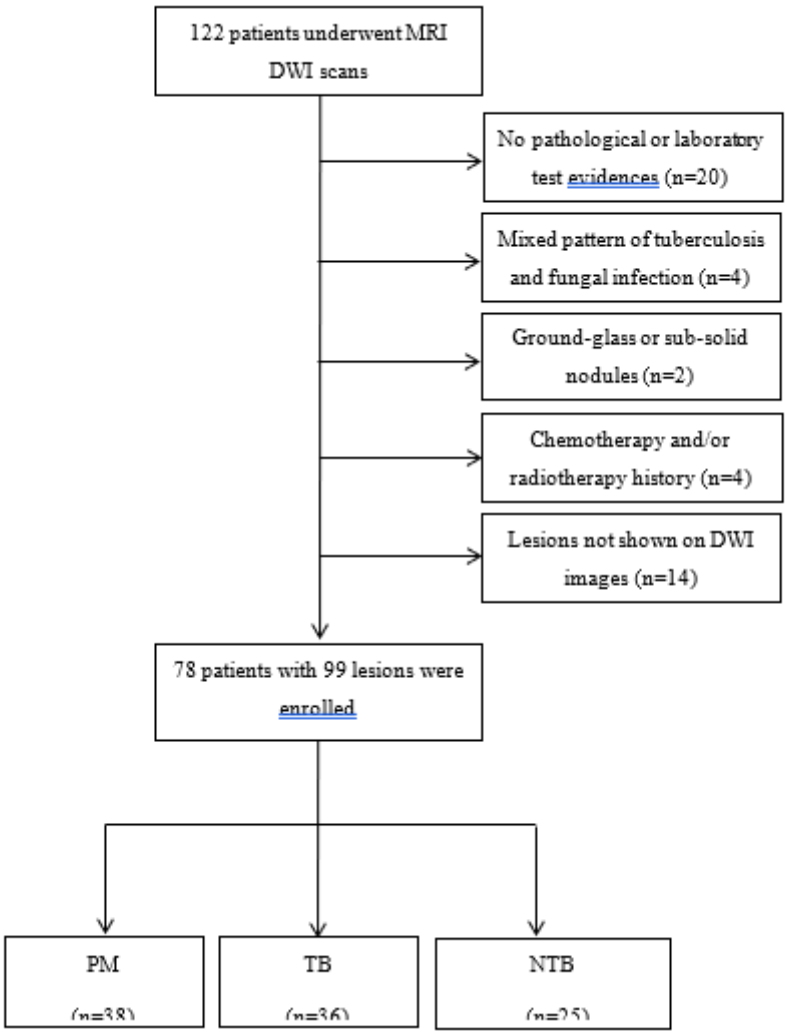

Figure 1

Enrollment of patients. Note: PM: pulmonary malignancy, TB: tuberculosis, NTB: non-tuberculosis benign lesions.

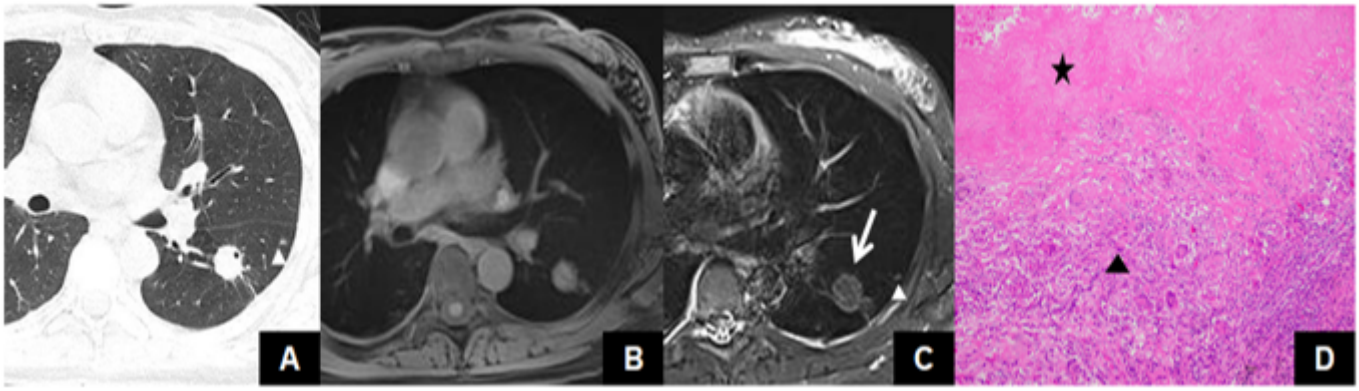

Figure 2

Figure 2 showed a tuberculoma in the lower lobe of the left lung. (white ▲) was satellite focus in CT(A) and T2WI fBALDE TSE images(C). The tuberculoma was slightly hyper-intensity in T1WI StarVIBE(B) and

central hypo-intensity with peripherally ring-like hyper-intensity in T2WI images, which was corresponding to the central caseous necrosis(□) and peripheral inflammatory granulomatous hyperplasia(black ▲) in the pathology(D).

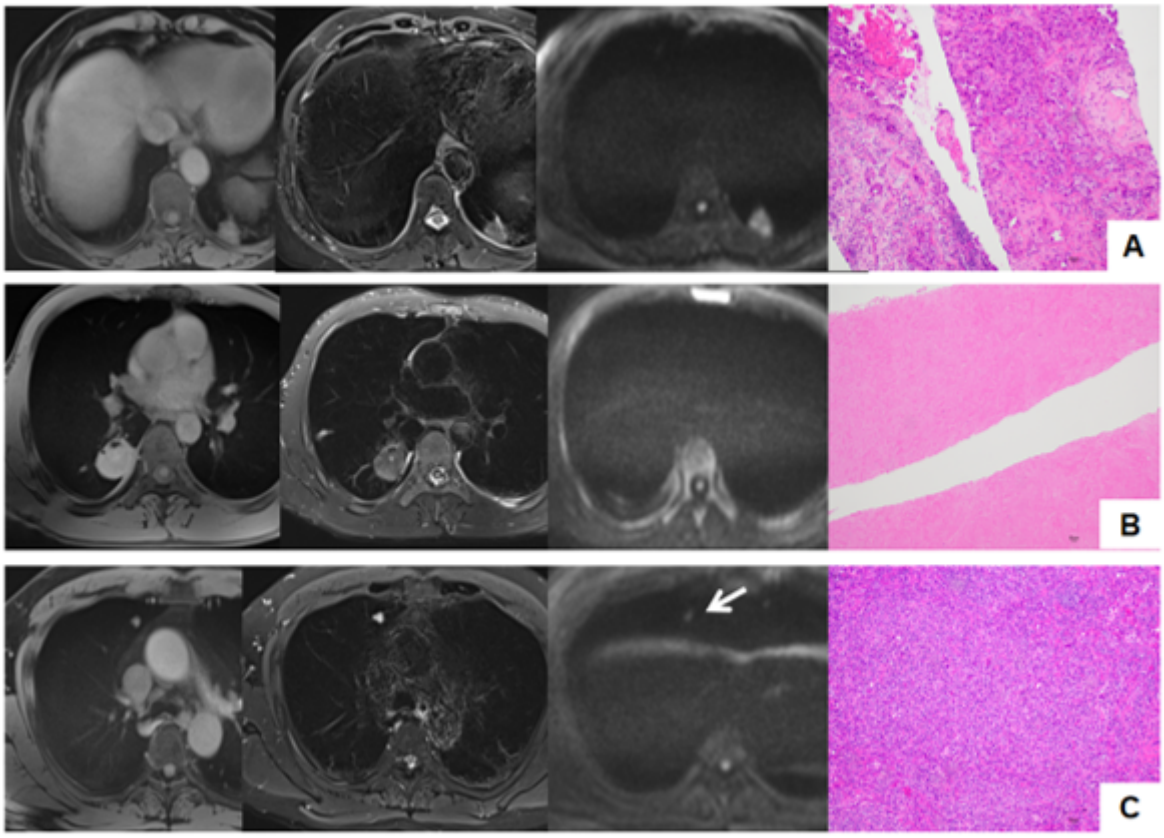

Figure 3

A. female, 60 years old. A adenocarcinoma in the lower lobe of left lung showed hyper-intensity in the T1WI StarVIBE, T2WI fBLADE TSE and DWI (b=1000 s/mm2) (from left to right in the first row). The ADC is 1.35 x 10-3 mm2/s. B. male, 42 years old. A tuberculoma in the lower lobe of the right lung showed slightly hyper-intensity in the T1WI StarVIBE (the first from the left in the second row) and slightly hypo-intensity in the T2WI fBLADE TSE (the second from the left in the second row). The DWI (the third from the left in the second row) showed no signal when b=1000 s/mm2. C. male, 56 years old. The inflammatory granuloma in the upper lobe of the right lung showed hyper-intensity in the T1WI StarVIBE, T2WI fBLADE TSE and DWI (b=1000 s/mm2) (from the left to the right in the third row). The ADC are 2.81 x 10-3 mm2/s.

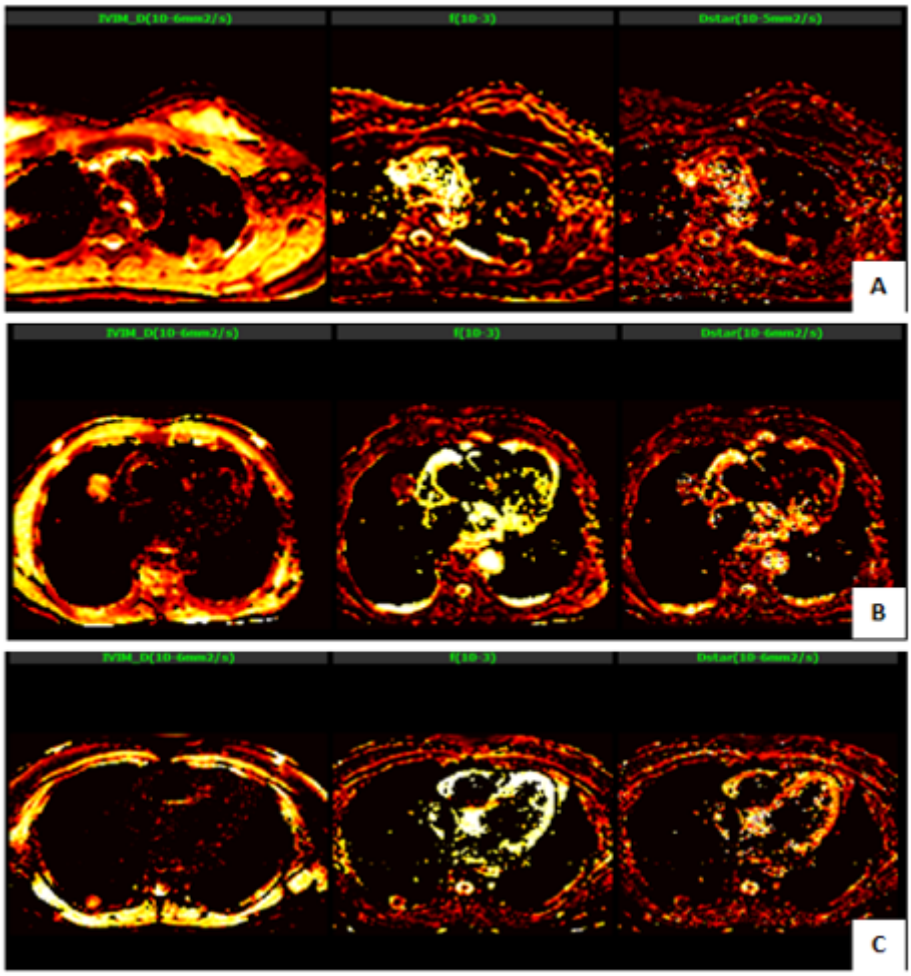

Figure 4

A. female, 39 years old, a tuberculoma in the upper lobe of left lung. IVIM D, D* and f are 1.51×10-3 mm2/s，11.92×10-3 mm2/s, 0.149. B. male, 62 years old, a adenocarcinoma in the lower lobe of right lung. IVIM D, D* and f are 1.10×10-3 mm2/s，18.94×10-3 mm2/s, 0.250. C. male, 39 years, a spherical pneumonia in the lower lobe of right lung. IVIM D, D* and f are 1.55×10-3 mm2/s，36.84×10-3 mm2/s, 0.215.

Supplementary Files

This is a list of supplementary files associated with this preprint. Click to download.

- Tables.docx